JOURNAL OF AIRCRAFT
Vol. 45, No. 1, January–February 2008

Tradeoff of Weight and Inspection Cost in Reliability-Based Structural Optimization

Amit A. Kale* and Raphael T. Haftka†
University of Florida, Gainesville, Florida 32611-6250

DOI: 10.2514/1.21229

This paper develops a methodology for cost-optimal, reliability-based structural design and inspection planning of aircraft structures subject to fatigue damage growth. An optimization problem is formulated to minimize the expected lifetime cost while maintaining a minimum acceptable reliability level. The effect of structural design and inspection schedule on operational cost and reliability is explored. The optimization parameters are the inspection times, types, and structural thickness. A computational technique using a combination of Monte Carlo simulation to estimate the crack size distribution after inspections and first-order reliability method to calculate failure probability at any time is developed to expedite reliability calculations. The paper shows that the simultaneous design of the structure and inspection regime allows trading the cost of additional structural weight against the inspection cost.

Nomenclature

a	=	crack size, mm
a_c	=	critical crack size, mm
a_h	=	inspection parameter, crack size at which probability of detection is 50%, mm
a_i	=	crack size at beginning of inspection interval, mm
$a_{i,0}$	=	crack size due to manufacturing defect, mm
a_N	=	crack size after N cycles of fatigue loading, mm
b	=	panel length, m
C_{kb}	=	cost of inspection schedule developed using kth inspection type, dollars
$C_{\min}$	=	minimum cost of inspection schedule, dollars
C_{tot}	=	total life cycle cost, dollars
cov	=	coefficient of variation, (standard deviation divided by mean)
D	=	Paris law parameter, $\text{m}^{1-\frac{m}{2}}$ $(\text{MPa})^{-m}$ and m is Paris law exponent
F_c	=	fuel cost per pound per flight, dollars
h	=	panel width, m
I_{ck}	=	cost of inspection of kth type, I_{c1}, I_{c2}, I_{c3}, I_{c4}, dollars
I_k	=	inspection of kth type, $k = 1, \ldots, 4$
K	=	stress intensity factor, $\text{MPa}\sqrt{\text{m}}$
K_{IC}	=	fracture toughness, $\text{MPa}\sqrt{\text{m}}$
l	=	fuselage length, m
M_c	=	material manufacturing cost per pound, dollars
m	=	Paris law parameter, Eq. (1)
N	=	number of cycles of fatigue loading, one cycle equals one flight for fuselage loading
N_f	=	fatigue life, flights
N_k	=	number of inspections of kth type in a schedule
N_{kb}	=	inspection schedule developed using only kth inspection type
N_p	=	number of panels
P_d	=	probability of detection
P_d^{rand}	=	random number for probability of detection
Pf_{th}	=	threshold probability of failure, reliability constraint
p	=	pressure differential, MPa
r	=	fuselage radius, m
S_l	=	service life (40,000 flights)
S_n	=	nth inspection time in number of cycles or flights (time, cycle, and flights are used interchangeably in this paper)
t	=	structural thickness, mm
W	=	fatigue controlled structural weight, lb
β	=	inspection parameter, Eq. (8)
ρ	=	density of aluminum, kg/m^3
σ	=	stress, MPa

Received 17 November 2005; revision received 29 November 2006; accepted for publication 2 January 2007.

*Graduate Research Assistant, Student, Department of Mechanical and Aerospace Engineering; akale@ufl.edu. Member AIAA.

†Distinguished Professor, Department of Mechanical and Aerospace Engineering; haftka@ufl.edu. Fellow AIAA.

I. Introduction

The integrity of structural components is affected by damage due to fatigue, corrosion, and accidental impact. Damage may reduce the residual strength of the structure below what is needed to carry the service loads. In a fail-safe design, structural safety can be maintained by inspecting the components and repairing the detected damage. Alternatively, stresses can be lowered by increasing structural sizes so that damage never grows to a critical length during service life: so-called safe-life design.

Structural component safety checks have gained widespread acceptance because of uncertainty in damage initiation and propagation. The damage tolerance approach to structural integrity assumes that damage is present in the structure at all times, and sufficient safety measures should be employed to ensure that it will not grow to a critical length during the operational life of the structure. The Federal Aviation Administration (FAA) requires that all structures designed for damage tolerance be demonstrated to avoid failure due to fatigue, environmental effects, manufacturing defects, and accidental damage.

It is easier to perform reliability-based structural optimization of safe-life structures than of fail-safe structures because the optimization of the former involves only structural sizes, whereas for the latter the inspection regime also needs to be optimized. Nees and Canfield [1] and Arrieta and Striz [2,3] performed safe-life structural optimization of F-16 wing panels to obtain the minimum structural weight for fatigue crack growth under a service load spectrum.

For aircraft fail-safe design, reliability-based design optimization has been applied to design the inspection schedules. Harkness et al. [4] developed an approximate method to evaluate reliability with inspections, Provan and Farhangdoost [5] used Markov chains to estimate the failure probability of a system of components, and Brot [6] demonstrated that using multiple inspection types could minimize cost.

Fujimoto et al. [7], Toyoda-Makino [8], Enright and Frangopol [9], Wu et al. [10], Garbatov and Soares [11], and Wu and Shin [12] developed optimum inspection schedules for a given structural

design to maintain a specified probability of failure. Wu and Shin [13] developed a methodology to improve the accuracy of reliability calculations with inspections.

Reliability-based optimization of the structural design and inspection schedules has also been applied to pipelines subjected to corrosion damage. Hellevik et al. [14] optimized the pipeline thickness together with the inspection regime to minimize the total operational cost. Using Bayesian updating and a decision tree, they obtained the optimum inspection regime in times and types of inspection. The corrosion information obtained from the inspection was used to update the corrosion model and corrosion probabilities.

Backman [15] also used multiple inspection types to develop an optimum inspection schedule. However, he also considered the tradeoff between the cost of inspection and the cost of additional structural weight for maintaining the same probability of failure. Using an approximate relationship between structural weight and damage propagation, he concluded that increasing the structural weight is more cost effective than increasing the inspection frequency.

Reliability-based design optimization (RBDO) is computationally very expensive when inspections are involved because crack size distribution has to be recharacterized after each inspection to simulate replacement. Calculation of structural reliability with inspection schedule has been done using Monte Carlo simulations (e.g., Brot [6], Enright and Frangopool [9] and Wu et al. [10]). Exact computation using Monte Carlo simulation (MCS) is very expensive for estimating a low probability of failure due to the large required sample size. For example, estimating failure probability of the order of 10^{-7} to 10% accuracy requires 10^9 samples. This makes it difficult to do the combined RBDO of structural design and inspection times using MCS alone. Harkness [16] developed a computational methodology to calculate reliability with inspections without updating the crack size distribution after each inspection. He assumed that repaired components will never fail again and incorporated this assumption by modifying the first-order reliability method (FORM).[‡] This leads to fast and accurate reliability computations that require only the specification of the initial crack size distribution. In previous papers (Kale et al. [17,18]), we used the same methodology to optimize the inspection schedule.

When inspections are scheduled before half of the service life, repaired components can have a large probability of failure. In this case, Harkness's method may not be accurate enough because the repaired components can fail during the remainder of the service life. To address the computational challenge of MCS and the accuracy problem of Harkness's method, we propose an approximate method to update the mean and standard deviation of the crack distribution after inspection and repair using MCS. MCS requires much fewer simulations to estimate mean and standard deviation than to estimate probability of failure. Subsequently, FORM is used to calculate the failure probabilities between inspections. The combined MCS and FORM approach to calculate failure probability with inspection removes the computational burden associated with calculating the failure probability using MCS for low failure probabilities.

The main objective of the present paper is to use this methodology to demonstrate the optimization of aircraft structural design together with inspection schedules. The optimization parameters are structural thickness, inspection times, and inspection types. The application of the proposed methodology is demonstrated by using an example of an aircraft structure modeled as an unstiffened panel designed for fatigue. A second objective of this paper is to demonstrate that if structures are designed together with the inspection schedule, then the cost of additional structural weight can be traded against the cost of additional inspections to achieve an overall minimum operational cost.

Section II of this paper describes the fatigue crack growth model and the inspection model used to determine optimum inspection schedules. This section also illustrates updating of crack size distribution after inspections. Section III describes the computation of the failure probability of a structure and determination of optimum inspection times and types for maintaining a minimum reliability level. Section IV discusses the combined optimization of inspections and structural sizes, and Sec. V presents the concluding remarks.

II. Structural Design and Damage Growth Model

A. Fatigue Crack Growth

We consider fatigue crack growth in a fuselage panel with an initial crack size a_i subjected to load cycles with constant amplitude. We assume that the main fatigue loading is due to pressurization, with stress varying between a maximum value of σ to a minimum value of zero in one flight. One cycle of fatigue loading consists of one flight. Like many other researchers (e.g., Tisseyre et al.,[§] Harkness et al. [4], Lin et al. [19]), we assume that damage growth follows the Paris equation

$$\frac{\mathrm{d}a}{\mathrm{d}N} = D(\Delta K)^m \tag{1}$$

where $\frac{\mathrm{d}a}{\mathrm{d}N}$ is the crack growth rate in m/cycle and the stress intensity factor range ΔK is in MPa$\sqrt{\mathrm{m}}$. For 7075-T651 aluminum alloy, D and m are material parameters related by Eq. (2) obtained from Sinclair and Pierie [20]. D has units in $\mathrm{m}^{1-\frac{m}{2}}$ $(\mathrm{MPa})^{-m}$

$$D = e^{(-3.2m-12.47)} \tag{2}$$

The stress intensity factor range ΔK for a center cracked panel is calculated as a function of the stress σ and the crack length a in Eq. (3), and the hoop stress due to the pressure differential p is given by Eq. (4):

$$\Delta K = \sigma\sqrt{\pi a} \tag{3}$$

$$\sigma = \frac{pr}{t} \tag{4}$$

The number of cycles of fatigue loading N accumulated in growing a crack from the initial crack size a_i to the final crack a_N can be obtained by integrating Eq. (1) between the initial crack a_i and the final crack a_N. Alternatively, the crack size a_N after N cycle of fatigue loading can be obtained by solving Eq. (5):

$$N = \int_{a_i}^{a_N} \frac{\mathrm{d}a}{D(\sigma\sqrt{\pi a})^m} = \frac{a_N^{1-(m/2)} - a_i^{1-(m/2)}}{D[1-(m/2)](\sigma\sqrt{\pi})^m} \tag{5}$$

The fatigue life of the panel can then be obtained by substituting the critical crack length a_c in place of a_N in Eq. (5):

$$N_f = \frac{a_c^{1-(m/2)} - a_i^{1-(m/2)}}{D[1-(m/2)](\sigma\sqrt{\pi})^m} \tag{6}$$

Here we assume that the critical crack length a_c is dictated by considerations of crack stability, so that

$$a_c = \left(\frac{K_{\mathrm{IC}}}{\sigma\sqrt{\pi}}\right)^2 \tag{7}$$

Typical material properties for 7075-T651 aluminum alloy are presented in Table 1. A conservative distribution of initial defects was chosen following the Department of Defense Joint Service Specification Guide, JSSG [21] for aluminum alloys to account for uncertainties in damage initiation and growth. The applied fuselage pressure differential is 0.06 MPa, obtained from Niu [22], and the stress is given by Eq. (4).

B. Inspection Model

When the structure is subjected to periodic inspections, cracks are detected and repaired or the structural part is replaced. We assume

[‡]FORM is a moment-based technique that calculates the failure probability using a first-order approximation about the point on the limit state closest to origin and is computational very cheap compared to MCS.

[§]Aerospatiale report obtained through private communication, 1991.

Table 1 Fatigue properties of 7075-T651 aluminum alloy, Sinclair and Pierie [20]

Property	Distribution type, mean, standard deviation
$a_{i,0}$, mm (mean, standard deviation)	Lognormal, 0.2, 0.07
m (mean, standard deviation)	Lognormal, 2.97, 1.05
Pressure load p, MPa (mean, standard deviation)	Lognormal, 0.06, 0.003
Fracture toughness K_{IC}, MPa$\sqrt{\text{m}}$	36.58, deterministic
Fuselage radius r, m	3.25, deterministic

that the probability P_d of detecting a crack of length a is given by Eq. (8) (Palmberg et al. [23]):

$$P_d(a) = \frac{(a/a_h)^\beta}{1 + (a/a_h)^\beta} \tag{8}$$

Values of a_h of 0.63, 0.80, and 1.27 mm were obtained from the probability of detection curves from Rummel and Matzkanin [24] for eddy current inspection and $a_h = 2.00$ mm was obtained from Tober and Klemmt [25] for ultrasonic inspection. The three versions of eddy current inspections differ in terms of the instruments used and the number of operators inspecting the component. They all obtained the probability of detection curves by artificially machining cracks in panels and counting the number of times that they were detected after being inspected. The value of the other inspection parameter β, as shown in Fig. 1, was obtained by fitting Eq. (8) to the inspection data in these references. The probability of detection curves for different inspection types are shown in Fig. 1. Type 1 is the most effective inspection followed by type 2, and so on. It is assumed that once a crack is detected, the panel is replaced by a newly manufactured panel with a smaller defect size distribution (fabrication defects).

III. Calculating an Inspection Schedule

A. Estimating the Crack Size Distribution After Inspection

When inspection and replacement of structural components are scheduled, the damage size distribution changes because defective parts are replaced with new parts having a smaller damage size (fabrication defects). Harkness [16] developed a computational methodology to calculate reliability with inspections without updating the crack size distribution after each inspection. He assumed that repaired components will never fail again and incorporated this assumption by modifying FORM. Using this method, FORM is updated over the failure region after each inspection using numerical integration. This expedites the reliability computations, which require only that the initial crack size distribution be specified. In previous papers (Kale et al. [17,18]), we used the same methodology to optimize the inspection schedule

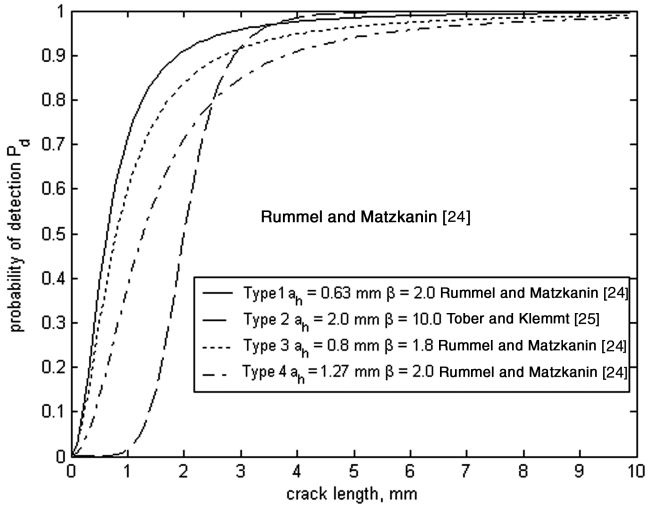

Fig. 1 Probability of detection curve for different inspection types from Eq. (8).

When inspections are scheduled after half the service life, this method gives accurate results because the repaired component will not fail until the end of service. However when inspections are scheduled before half of the service life, the repaired components can have a large probability of failure and Harkness's method may not be accurate enough. We have the option of using MCS to update damage distribution as well as to calculate the probability of failure, but for low probability of failure this would be very expensive computationally. For example, for a 10% accuracy, estimating a probability of failure of 10^{-7} requires 10^9 simulations.

Kale et al. [26] developed an approximate method to account for inspection and repair using MCS, but evaluating the failure probability using FORM. The computational savings are realized by assuming a distribution type for the damage sizes and using MCS only to estimate the mean and standard deviation of the probability distribution after each inspection and repair. This requires a much smaller sample size. Then FORM is used to calculate the failure probabilities at any time following the inspection. This greatly expedites the reliability computations. A comparison between Harkness's method [16] with the proposed approach in Appendix C demonstrates the large possible errors associated with Harkness's method and the improved accuracy using the present approach.

Here we assume that inspections do not change the type of distribution and that damaged components are replaced by new components with damage distribution due to fabrication. The damage distribution after an inspection can easily be updated by using MCS with a small sample size. The crack size a_N after N cycle of fatigue loading is obtained by solving Eq. (5). To obtain the crack size mean and standard deviation after an inspection is conducted, we produce 100,000¶ random numbers for each random variable in Eq. (5) (a_i, m, σ) and obtain the final crack size a_N. We then simulate the inspection by using Eq. (8) with another random number for probability of detection. If the crack is detected, the panel is replaced by a new one with a random crack size picked from the distribution of manufacturing defects $a_{i,0}$. After all cracks are analyzed for detection, the updated crack sizes are used to fit a distribution and to obtain its mean and standard deviation. This serves as the initial crack distribution for the next inspection. For the data used in this paper, the fabrication crack distribution is lognormal, and the distribution after inspections was also found to be best approximated by lognormal distribution out of 12 analytical distributions in ARENA software© [27]. If better accuracy is needed then a distribution with more parameters can be fitted to the data. And so in general, the present approach can be used with the MCS used to fit a new distribution for the crack sizes after each inspection. The pseudocode for updating crack distribution after N cycles from previous inspection is shown as follows:

1) Generate a panel by a random vector of uncertain variables (a_i, m, σ).

2) Solve Eq. (5) for crack size a_N after N cycles of fatigue loading corresponding to the random vector (a_i, m, σ).

3) Compute the probability of detection of crack a_N from Eq. (8), $P_d(a_N)$.

4) Generate a random number from a uniform distribution with bounds (0, 1) P_d^{rand}.

5) If $P_d(a_N) \geq P_d^{\text{rand}}$ then simulate replacement of defective component by generating a random crack $a_{i,0}$ for a new panel and set $a_N = a_{i,0}$, else keep a_N.

6) Store a_N for fitting probability distribution to crack sizes after inspection.

¶A large sample size was used to get accurate estimate of mean and standard deviation. This makes the optimization results insensitive to MCS seed. For a given problem the uncertainty in mean and standard deviation due to finite sample size can be calculated and the size of MCS can be increased to get a desired level of accuracy.

Table 2 Example 1, inspection schedule and crack size distribution after inspection ($a_h = 0.63$ mm) for an unstiffened plate thickness of 2.48 mm and a threshold probability of 10^{-7}

No. of inspections	Inspection time (flights)[a]	Inspection interval (flights), $S_n - S_{n-1}$	Crack size distribution after inspection (mean, mm, cov)
0	——	——	Initial crack distribution (0.200, 0.35)
1	14,569	14,569	(0.264, 1.04)
2	26,053	11,484	(0.271, 1.11)
3	35,576	9,523	(0.245, 1.10)

[a]Inspection times may differ by a maximum value of 100 flights due to MCS seed; the corresponding error in probability calculation is negligible.

7) Stop after 100,000 random panels have been simulated and fit distribution to crack sizes.

B. Calculating the Failure Probability Using FORM

It would be possible to use the same MCS procedure as described in the preceding step to calculate the probabilities of failure needed for scheduling inspections (e.g., Enright and Frangopol [9] and Wu and Shin [12,13]). However, because the required probabilities of failure are of the order of 10^{-8}, this would require a prohibitively large MCS. Instead we use FORM, taking advantage of the characterization of the crack distribution as lognormal, as described in the preceding section. The probability of failure after N cycles of fatigue loading since the most recent inspection is

$$P_f(N, a_i) = P[a(N, a_i) \geq a_c] \tag{9}$$

where a_i is the crack size distribution (either initial or updated) at the beginning of the inspection period and a_c is the critical crack given by Eq. (7). This probability is calculated by FORM. For a given structural thickness, optimum inspection times are obtained such that the probability of failure before the inspection is just equal to the maximum allowed value (Pf_{th}, reliability constraint). The probability of failure decreases after the inspection, because cracks are detected and repaired. With the number of cycles of loading (flights), the failure probability increases until it hits the threshold value again, defining the next inspection. The nth inspection time S_n is obtained by solving Eq. (9) using a bisection method between the previous inspection time** S_{n-1} and the service life S_l (40,000 flights). To ascertain whether the number of inspections is adequate, the probability of failure at the end of service is calculated. If this failure probability is greater than the threshold value, additional inspections must be added. The combined MCS and FORM approach removes the computational burden associated with calculating the failure probability using MCS for very low failure probabilities.

To demonstrate the application of the combined FORM and MCS method to calculate the failure probability, we calculate the inspection time for a 2.48 mm fixed structure for a threshold reliability level of $Pf_{\text{th}} = 10^{-7}$ in Table 2. Calculating using FORM in Eq. (9) with $a_i = a_{i,0}$ and solving for N, the first inspection time is 14,569 flights. To update the crack size distribution after this inspection, crack growth simulation using the MCS pseudocode is performed with initial crack sizes $a_{i,0}$ and a crack growth time of 14,569 flights. This gives the updated crack size distribution after the first inspection a_i (mean = 0.264 mm, cov = 1.04). This serves as the initial crack size distribution for the second inspection. The second inspection time is obtained by solving Eq. (9) using FORM with the updated initial crack size distribution a_i (mean= 0.264 mm, cov = 1.04). This is continued until the failure probability at the end of service life is less than the specified value.

Figure 2 illustrates the variation of the probability of failure with and without inspection. It can be seen that inspections are very helpful in maintaining the reliability of the structure. From Table 2 it can be seen that the first inspection interval is the largest. After the first inspection, damaged components are replaced with the same initial crack distribution (mean = 0.20 mm and cov = 0.35); however, some cracks may have escaped detection. The fact that some cracks (larger than the initial cracks) may have escaped detection and will grow faster leads to smaller intervals.

In Table 2 we see that the crack size distribution has a large coefficient of variation (greater than 1.0) at each inspection compared to the initial crack size distribution (cov = 0.35). The reason of large cov is the nonlinear nature of crack growth. The crack grows according to the power law [Eq. (5)], which means that small cracks grow slowly and large cracks grow faster. This creates a large scatter in the crack size distribution as the cracks grow with time, leading to high cov.

The preceding example showed how an optimum inspection schedule can be developed for a single inspection type. The same procedure is followed for scheduling the inspection sequence with multiple inspection types. Here the probability of detection of each inspection type can be different, and inspections are performed in the same order as specified in the sequence. If the specified reliability level cannot be maintained with the inspection sequence, then it is not feasible.

C. Cost Model

The cost associated with a change in the structural weight for aluminum and the fuel cost is taken from Venter [28]. He assumed a fuel cost of \$0.89 per gallon and calculated that a pound of structural weight will cost 0.1 lb of fuel per flight. From this we calculate that a pound of structural weight will cost \$0.015 in a flight for fuel. The structural weight is assumed to be directly proportional to the plate thickness and a pound of structural weight is assumed to cost \$150 for material and manufacturing. Appendix B shows the details of material and fuel cost calculations. A typical inspection cost of about a million dollars was obtained from Backman [15] and costs of other inspection types were adjusted such that the incentive for carrying less effective inspection decreases with the number of inspections. Thus, one inspection of the first type is more attractive than carrying two inspections of the second type, three inspections of the third type, or four inspections of the fourth type. The structural design

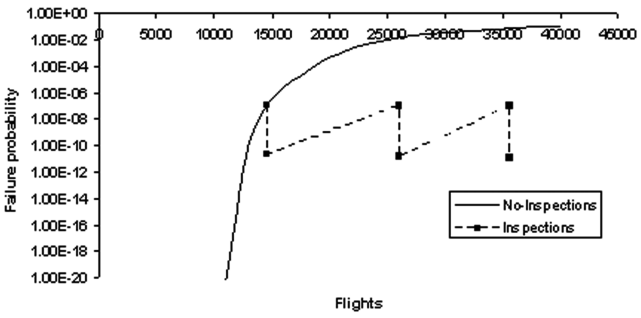

Fig. 2 Variation of failure probability with number of cycles for a 2.48 mm thick unstiffened panel with inspections scheduled for $Pf_{\text{th}} = 10^{-7}$.

**Time, cycle, and flights are used interchangeably in this paper because for one cycle of fatigue loading is equal to one flight in a fuselage and time is measured in number of flights.

Table 3 Design details and cost factors, Venter [28] and Backman [15]

Variable	Value
Density of aluminum ρ	2670 $\frac{kg}{m^3}$
Frame spacing b	0.6 m
Fuel cost per pound per flight F_c	\$0.015
Fuselage radius r	3.25 m
Fuselage length l	68.3 m
Material and manufacturing cost per pound M_c	\$150.0
No. of panels N_p	1350
Panel width h	1.72 m
Type 1 inspection cost I_{c1}	\$1.35 million
Type 2 inspection cost I_{c2}	\$1.23 million
Type 3 inspection cost I_{c3}	\$0.98 million
Type 4 inspection cost I_{c4}	\$0.85 million

parameters for the B747 series aircraft obtained by Niu [22] are also listed in Table 3. Following Backman [15] the service life is assumed to be 40,000 flights.

The life cycle cost is calculated as

$$C_{\text{tot}} = M_c W + F_c W S_l + \sum_{k=1}^{4} I_{ck} N_k \tag{10}$$

$$W = N_p thb\rho \tag{11}$$

During the optimization, the structural thickness t changes; this in turn changes the structural weight according to Eq. (11). The optimum inspection schedule (times and types) is determined for this structural design and the total cost is obtained from Eq. (10).

D. Optimization of Inspection Types

The combined optimization of inspection times to minimize the cost for the specified reliability constraint is complicated because of the large number of permutations of inspection types that can occur in an inspection schedule. To reduce the number of permutations that need to be considered, we first calculate the inspection schedule and the cost of all the single-type inspections. We then use the lowest cost as a bound that allows us to eliminate many possible sequences. Appendix A provides a detailed description of the algorithm.

1) Determine optimum inspection times and costs using each of the four inspection types. This step provides (N_{kb}, C_{kb}), where N_{kb} is the number of required inspections of the kth type (i.e., if only type k is used) and C_{kb} is the total cost of an inspection schedule developed using only the kth inspection type. Determine the minimum cost, $C_{\min} = \min(C_{\text{kb}}, k = 1, \ldots, 4)$.

2) Eliminate impossible or clearly suboptimal inspection sequences to seek a mix of inspection types with N_k inspections of type k. If we use more than one inspection type, the total number of inspections in the sequence should be at most equal to the number of inspections required by the least effective inspection in the sequence. Also, the total number should be at least equal to the number of inspections required by most effective inspection in the sequence:

$$\min_{N_k \neq 0}(N_{\text{kb}}) \leq \sum_{k=1}^{4} N_k \leq \max_{N_k \neq 0}(N_{\text{kb}}) \tag{12}$$

$$N_k < \left\lfloor \frac{C_{\min}}{I_{\text{ck}}} \right\rfloor \tag{13}$$

3) Generate the cheapest inspection sequence satisfying Eqs. (12) and (13). Generate all possible inspection-type sequences by permuting the order of inspection types as described in Appendix A.

4) Generate the inspection times for the inspection sequence and check if the failure probability at the end of the service life is less than the specified reliability constraint. (i.e., whether the inspection sequence is feasible). If multiple inspection-type sequences are feasible, select the one with lowest probability of failure at the end of service life.

5) Stop if the sequence is feasible, otherwise generate the next cheapest inspection sequence and go back to step 4.

IV. Combined Optimization of Structural Design and Inspection Schedule

Our objective is to determine the optimum combination of the structural thickness, inspection types, and inspection times that lead to a minimum life cycle cost for maintaining the specified reliability level (Pf_{th}) through the service life. To obtain the optimum thickness we first obtain the safe-life thickness, which is the minimum thickness necessary to maintain the threshold probability of failure without any inspection. To determine whether additional inspections reduce cost, we do a 1-D search on the thickness by reducing the thickness gradually and obtain optimum inspection schedule using the algorithm described in Sec. III until we get the optimum lifetime cost.

A. Safe-Life Design

When inspections and maintenance are not feasible, safety can be maintained by having a conservative (thicker) structural design. To demonstrate this, we first obtain the safe-life design required to maintain the desired level of reliability throughout the service life. Table 4 shows the safe-life design.

From Table 4, comparing the minimum thickness to that used in Example 1 (Table 2), we see that the safe-life design must be very thick and heavy to maintain the required safety levels.

B. Cost Effectiveness of Combined Structural Design and Inspection Schedule Optimization

Next we demonstrate the effect of inspections on structural safety and operational cost. Inspections improve the reliability by detecting and removing cracks. If this effect is used to optimize the structural design together with the inspection schedule, then the structural weight could be traded against the inspection cost to reduce the overall operational cost. The results of combined structure and inspection optimization are shown in Table 5.

From Table 5 we can see that if inspections are added, the structural thickness can be reduced to maintain the required reliability level at a lower cost. Inspections are very useful in maintaining the structural safety in that large cracks are detected and the damaged part is replaced with new components, improving the fatigue life. In this paper we optimize the inspection schedule for fatigue damage. However, inspections are also used to detect other damage, such as tool drop, bird impact, and corrosion, which makes them even more cost effective compared to the safe-life design.

Table 4 Safe-life design

Threshold probability of failure, Pf_{th}	Minimum required skin thickness, mm	Life cycle cost, $\times 10^6$	Structural weight, lb	% increase in cost of improving reliability by a factor of 10
10^{-7}	4.08	25.42	33,902	——
10^{-8}	4.20	26.16	34,880	2.91
10^{-9}	4.24	26.34	35,129	0.68

Table 5 Optimum structural design and inspection schedule

Threshold probability of failure, Pf_{th}	Optimum plate thickness, mm	Optimum inspection type sequence	Optimum inspection time (flights)	Minimum cost, $\times 10^6$	Cost factors, %		
					F_c	M_c	I_c
10^{-7}	2.48	I_1, I_4, I_3	14,569, 26,023, 32,706	18.66	66	16	18
10^{-8}	2.54	I_1, I_3, I_1	14,321, 23,780, 30,963	19.47	64	16	20
10^{-9}	2.66	I_1, I_3, I_1	15,064, 23,532, 30,023	20.27	65	16	19

Table 6 Comparison of optimum inspection schedule using a single inspection type for a fixed structural size

Threshold probability of failure, Pf_{th}	Optimum plate thickness, mm	Optimum inspection-type sequence using a single inspection type				Minimum cost, $\times 10^6$
		I_1	I_2	I_3	I_4	
10^{-7}	2.48	14,569, 26,053, 35,576	14,569, 24,683, 33,430	14,569, 19,596, 29,502, 35,156	14,569, 18,991, 25,952, 30,128, 38,167	I_2: 19.17
Inspection cost, $\times 10^6$		4.05	3.69	3.92	4.25	

Table 7 Optimum structural design and inspection schedule using only a single inspection type

Threshold probability of failure, Pf_{th}	Optimum plate thickness, mm	Optimum inspection time (flights)	Optimum inspection type	Minimum cost, $\times 10^6$
10^{-7}	2.39	13,317, 18,651, 26,642, 32,460	I_3	18.78
10^{-8}	2.50	13,971, 22,897, 31,443	I_1	19.65
10^{-9}	2.64	14,975, 19,642, 26,230, 32,670	I_3	20.41

Table 8 Optimum structural design (plate thickness of 2.02 mm) and inspection schedule for $Pf_{th} = 10^{-7}$ for doubled fuel cost

Inspection-type sequence	Optimum inspection time (flights)	Minimum cost, $\times 10^6$
I_1	9,472, 14,383, 20,204, 25,583, 31,192, 36,623	30.71
I_2	9,472, 13,431, 17,315, 21,659, 26,191, 30,784, 35,359, 39,917	32.45
I_3	9,472, 11,290, 17,422, 20,206, 25,773, 29,006, 34,178, 37,711	30.45
I_4	9,472, 11,001, 14,575, 17,130, 21,277, 24,231, 28,099, 31,225, 34,907, 38,178	31.11
$I_1, I_3, I_3, I_3, I_3, I_3, I_3$ (optimum schedule)	9,472, 14,383, 18,120, 22,941, 26,770, 31,495, 35,433	29.84

The combined optimization of structural design and inspection schedule leads to tradeoff of the costs of structural weight against the inspection cost. Comparing Tables 4 and 5, we can see that adding inspection leads to a 25% saving in life cycle cost over the safe-life design. Also, we can see that as the safety requirement becomes more stringent, additional and/or more effective inspections become worthwhile. For a safety level of 10^{-7}, cheaper inspections can be used (I_4 and I_3), whereas for 10^{-9} more effective inspections are useful. We can see that only a single inspection type may not be the best choice for maintaining different reliability levels. For maintaining a reliability level of 10^{-7}, a structural size of 2.48 mm and three inspections of types 1, 4, and 3 leads to minimum cost, but the same choice of inspection types is not suitable for a reliability level of 10^{-8}. The last columns of Table 5 show the cost factors in percentage of fuel cost F_c, manufacturing cost M_c, and inspection cost I_c. It can be seen that the fuel cost is the major design driver and more inspections can be used to tradeoff cost if fuel cost increases. This issue is further explored in the following section.

Next we compare the optimum inspection schedule developed using only a single inspection type for the structural thickness obtained in Table 5 for a reliability level of 10^{-7}.

Table 6 shows the inspection schedules and cost for the inspection sequence generated using individual inspection types for a fixed structural size. Comparing Tables 5 and 6, it can be seen that for a fixed structure, multiple inspection types can reduce cost. For a given structure, the advantage of multiple inspection types is partly driven by the fact that at the end of the service life, each inspection schedule leads to a different probability of failure. That is, the cost differential is partly due to different safety margins at the end of service. With combined structural and inspection optimization, the margin at the end of the service life is removed by a reduction in structural thickness. This leads to a smaller incentive for multiple inspection types, as shown in Table 7.

Comparing Tables 5 and 7 we can conclude that mixing inspections leads to only a small improvement in cost over a single inspection-type design (1.0%) when structural optimization is done with inspection scheduling.

C. Effect of Fuel Cost

Fuel cost has a large effect on the optimization of the structural design and inspection schedule. To demonstrate the effect of the increase in fuel cycle cost since 1998, we double the fuel cost to \$1.8 per gallon or \$0.03 per pound per flight. For the optimum design in Table 5, the fuel cost is about 60% of the total life cycle cost and inspections accounted for 20%. Optimization of the structural design and inspection schedule is performed for a reliability level of 10^{-7}. The optimum plate thickness is 2.02 mm and a comparison of the optimum inspection schedule using different inspection sequences is shown in Table 8.

Comparing Table 8 to the first row of Tables 5 and 6, we can conclude that as fuel cost increases it becomes advantageous to schedule additional inspections and reduce weight to reduce the overall life cycle cost. For the optimum structural design and inspection schedule in Table 8, the fuel cost is 66%, the manufacturing cost 8%, and inspections are 26% of the total cost. It should be noted, however, that fatigue is not the only structural design driver, so that at lower thicknesses, other structural constraints may dominate.

V. Conclusions

A methodology for developing optimum inspection-type sequences, time, and structural thickness was developed for fuselage panels. Uncertainty in material properties, crack sizes, and loads were considered. The FORM method was used to determine the probability of failure at a given time and crack size distribution after inspection was updated using Monte Carlo simulation. The methodology resolved the problem of very high computational cost when Monte Carlo simulations are used exclusively and the accuracy problem associated with the assumptions needed to allow exclusive use of FORM. Inspections and structural sizes were optimized so that a given threshold probability of failure was never exceeded. The study led to the following conclusions:

1) Combined structural and inspection optimization permits trading off inspection costs against the cost of structural weight, leading to reductions in overall lifetime cost. From the example used in this paper, about 25% saving in cost and weight can be achieved by using inspections.

2) Inspections are very cost effective. Even if only their effect on fatigue is considered, they can lead to substantial reductions in lifetime cost. Their advantages for detecting other types of damage, such as that due to corrosion, tool drops, and accidental impact, only add to their usefulness.

3) Combined optimization of structural weight and inspection reduces the lifetime cost penalty associated with single type of inspection, thus allowing possible simplification of the inspection regime.

4) Because fuel cost is the dominant cost associated with structural weight, increases in fuel cost drive the optimum designs towards more inspections and lower structural weight.

Appendix A: Optimization of Mix of Inspection Types

Optimization of an inspection schedule with different inspection types is computationally time-consuming because the inspection time and type of each subsequent inspection depends on the inspection time and type of previous inspections. As an illustration, if four inspection types are to be chosen to schedule, four inspections for minimum cost, this will require a reliability analysis on $4 \times 4 \times 4 \times 4 = 256$ different type sequence. However, in a typical optimization problem, the number of inspections required to satisfy reliability constraint is unknown and is obtained directly from reliability analysis (optimization of inspection times for fixed reliability). The computational cost may be prohibitive if a brute force approach is used. We seek a mix of inspection types and reduce the number of sequence by eliminating impossible or clearly suboptimal inspection types. The terminology used in the algorithm is described as follows:

1) *Baseline inspection schedule* (N_{kb}, C_{kb}): Optimum number of inspections of kth type and N_{kb} and the corresponding cost C_{kb} if only the kth inspection type is used to optimize the inspection schedule for a given reliability constraint.

2) *Combination sequence*: Number of inspection of each type that can be used to generate the inspection schedule (time of inspection). For example, a combination represented by $[N_1 = 1,\ N_2 = 2,\ N_3 = 1,\ N_4 = 2]$ means that there is one inspection of type 1, two inspections of type 2, one inspection of type 3, and two inspections of type 4 in an inspection schedule. In all of them there are six inspections available to generate the inspection schedule

3) *Inspection-type sequence*: The order in which the various inspections are done. For example, a combination sequence represented by $[N_1 = 0,\ N_2 = 1,\ N_3 = 1,\ N_4 = 1]$ can have six different orders in which an inspection of each type can be conducted. These are 1) I_2, I_3, I_4, 2) I_2, I_4, I_3, 3) I_3, I_2, I_4, 4) I_3, I_4, I_2, 5) I_4, I_2, I_3, 6) I_4, I_3, I_2. The order of the inspection type is important in generating the optimum inspection schedule for minimum cost, because the reduction in the probability of failure of one sequence can be different from others, P_d being a function of crack size and crack size being a function of time.

4) *Constraint 1*: $N_k < \lfloor \frac{C_{\min}}{I_{\mathrm{ck}}} \rfloor$, where [ ] is a rounded-up integer. This constraint essentially means that the maximum number of inspections of the kth type that can occur in a combination sequence should be such that the cost due to inspection of the kth type is less than or equal to the minimum cost $C_{\min}$.

5) *Constraint 2*: $N_{1b} < \sum_{k=1}^{4} N_k < N_{4b}$ The reason for this constraint is that N_{1b} is the optimum number of inspections obtained using the most effective inspection type. A total number of inspections in a combination sequence $\sum_{k=1}^{4} N_k$ less than N_{1b} is a direct violation of the reliability constraint. N_{4b} is the optimum number of inspections obtained using the least effective inspection type. The total number of inspection in a combination sequence $\sum_{k=1}^{4} N_k$ greater than N_{4b} is a direct violation of the cost constraint.

Appendix B: Calculation of Material Cost

Fuel cost and material manufacturing cost may account for more than 80% of the total life cycle cost. In this paper we calculate the fuel cost based on data obtained from Venter [28]. The fuel cost is assumed to be \$0.89 per gallon and it is assumed that a pound of structural weight will cost 0.1 lb of fuel in a flight. This leads to a fuel cost of \$0.0134 per pound per flight (assuming a gallon of jet fuel weighs 6.7 lb). In this paper, a slightly higher value of \$0.015 per pound per flight is used for convenience.

The material manufacturing cost was obtained by scaling down the material cost of the composite (\$250) from Venter [28] to \$150 per pound for aluminum from our previous paper (Kale et al. [17]). The scaling down is based on a rough estimate only to demonstrate the methodology rather than performing true cost calculation. The rough cost estimate of about \$110 per pound was obtained from Petit et al. [29]. They obtained the cost estimate for stiffened metallic fuselage panels for the B777 series aircraft. The structure used in Petit et al. consists of a 3.04×3.04 m^2 structural component with 14 stringers, 7 frames, and 7 fail-safe straps bonded to each frame. The fuselage length is $l = 62$ m, the radius is $r = 3.2$ m, and the skin thickness is 1.6 mm. The total manufacturing cost for the fuselage structure is \$2.78 million. The computation of the total volume of a single structural component for weight calculation is given in Table B1.

Single panel area $= 9.24$ m^2. The total fuselage surface area is $2\pi rl = 1246$ m^2; this corresponds to 135 panels.

The skin panel volume is skin area times thickness$= 9.24 \times 0.0016$ m^3.

Aluminum density $\rho = 2670$ kg/m^3.

Total fuselage weight = number of panels $\times$ (stringer volume+ frame volume + strap volume + skin volume) $\times\ \rho = 11512$ kg.

Cost per unit weight $= \frac{2{,}780{,}000}{11{,}512} = 241$ per kg or \$110 per pound.

Appendix C: Comparison of Methods of Reliability Computation

This Appendix compares the method of reliability calculation for inspection schedule developed by Harkness [16] with the methodology proposed in this paper. The moment-based method developed by Harkness simplifies the probability calculation by

Table B1 Area of structural dimensions for cost calculation, Petit et al. [29]

Structural component	Area, m^2	No. of components	Total area, m^2	Total volume, m^3 (Total area $\times$ Width)
Stringer	2×10^{-4}	14	28×10^{-4}	85.64×10^{-4}
Frame	3×10^{-4}	7	21×10^{-4}	63.84×10^{-4}
Tear strap	0.96×10^{-4}	7	6.77×10^{-4}	20.48×10^{-4}

Table C1 Inspection schedule and crack size distribution after inspection ($a_h = 0.63$ mm) for a 2.0 mm thick plate and a threshold probability of 10^{-6} developed using Harkness's method

No. of inspections	Inspection time (flights)	Failure probability calculated by Harkness's method	Actual failure calculated by MCS
0	——	——	——
1	9,908	10^{-6}	6.20×10^{-7}
2	22,830	10^{-6}	9.83×10^{-4}
End of service	40,000	1.0×10^{-7}	2.15×10^{-2}

Table C2 Inspection schedule and crack size distribution after inspection ($a_h = 0.63$ mm) for a 2.0 mm thick plate and a threshold probability of 10^{-4} developed using Harkness's method

No. of inspections	Inspection time (flights)	Failure probability calculated by Harkness's method	Actual failure calculated by MCS
0	——	——	——
1	11,664	10^{-4}	7.14×10^{-5}
2	29,668	10^{-4}	2.95×10^{-2}
End of service	40,000	5.4×10^{-8}	1.04×10^{-4}

Table C3 Inspection schedule and crack size distribution after inspection ($a_h = 0.63$ mm) for a 2.0 mm thick plate and a threshold probability of 10^{-6} developed using the proposed method

No. of inspections	Inspection time (flights)	Failure probability calculated by proposed method	Actual failure calculated by MCS	Crack size distribution after inspection (mean, mm, cov)
0	——	——	——	Initial crack distribution (0.200, 0.35)
1	9,908	10^{-6}	5.60×10^{-7}	(0.272, 1.04)
2	16,298	10^{-6}	4.61×10^{-6}	(0.260, 1.05)
3	22,914	10^{-6}	9.00×10^{-7}	(0.255, 1.06)
4	29,470	10^{-6}	1.16×10^{-6}	(0.252, 1.07)
5	36,020	10^{-6}	1.06×10^{-6}	(0.250, 1.07)
End of service	40,000	9×10^{-8}	$<1.00 \times 10^{-8}$	——

Table C4 Inspection schedule and crack size distribution after inspection ($a_h = 0.63$ mm) for a 2.0 mm thick plate and a threshold probability of 10^{-5} developed using the proposed method

No. of inspections	Inspection time (flights)	Failure probability calculated by proposed method	Actual failure calculated by MCS	Crack size distribution after inspection (mean, mm, cov)
0	——	——	——	Initial crack distribution (0.200, 0.35)
1	11,664	10^{-4}	7.00×10^{-5}	(0.272, 1.09)
2	22,709	10^{-4}	1.54×10^{-4}	(0.260, 1.30)
3	32,653	10^{-4}	8.36×10^{-5}	(0.244, 1.28)
End of service	40,000	1.10×10^{-5}	1.17×10^{-5}	——

assuming that repaired components will not fail. This assumption can be easily incorporated in FORM to calculate failure probability and provides accurate results if inspections are scheduled after 50% of service life (Harkness). When inspections occur before 50% of service life, the FORM method the repaired components may have large probability of failure before the end of service. Here, Harkness's method will underestimate failure probability.

To compare the two approaches we calculate the inspection schedule using 1) Harkness's method and 2) the method proposed in this paper, and calculate the failure probability at the inspection times using MCS with 5×10^7 samples. First we calculate the inspection times for a 2.0 mm thick plate, necessary to maintain a threshold reliability level of 10^{-6} and 10^{-4} using the method developed by Harkness (repaired cracks never fail) and calculate the probability of failure at these inspection times using MCS with 5×10^7 samples. The reliability level of 10^{-6} is chosen because it is close to a reasonable target reliability, but for that level MCS has substantial errors. The reliability level of 10^{-4} allows us to obtain MCS results that are accurate to about 2%.

Tables C1 and C2 show that at the first inspection the Harkness method is reasonably accurate, with the error coming from the FORM approximation. However, after repair (second inspection) the actual failure probability calculated by large MCS simulation (5×10^7 samples) is much higher than that calculated by Harkness's method. Tables C3 and C4 show similar calculations for the method proposed in the present paper. Comparing Tables C1 and C2 to Tables C3 and C4, we note that both methods give the same values at the first inspection, because both use FORM for probability calculations. The difference between the MCS values in the tables for the first inspections gives us a measure of the scatter in the MCS calculations. After the first inspections the tables diverge, with the results of the proposed method being much more accurate.

Acknowledgment

This research is supported by the NASA Constellation University Institute Project, CUIP (formerly University Research Engineering and Technology Institutes, URETI) Grant NCC3-994 to the Institute for Future Space Transport (IFST) at the University of Florida and NASA Grant NAG1-02042.

References

[1] Nees, C. D., and Canfield, R. A., "Methodology for Implementing Fracture Mechanics in Global Structural Design of Aircraft," *Journal of Aircraft*, Vol. 35, No. 1, 1998, pp. 131–138.

[2] Arietta, A. J., and Striz, A. G., "Modelling of Aircraft Fatigue Load Environment," AIAA Paper 00-0973, 2000.
[3] Arietta, A. J., and Striz, A. G., "Optimal Design of Aircraft Structures with Damage Tolerance Requirements," *Structural and Multidisciplinary Optimization*, Vol. 30, No. 2, 2005, pp. 155–1631.
[4] Harkness, H. H., Fleming, M., Moran, B., and Belytschko, T., "Fatigue Reliability Method with In-Service Inspections," *FAA/NASA International Symposium on Advanced Structural Integrity Methods for Airframe Durability and Damage Tolerance, NASA Conference, Part 1*, NASA Langley Research Center, Hampton, VA, 1994, pp. 307–325.
[5] Provan, J. W., and Farhangdoost, K., "A New Stochastic Systems Approach to Structural Integrity," *FAA/NASA International Symposium on Advanced Structural Integrity Methods for Airframe Durability and Damage Tolerance, NASA Conference, Part 1*, NASA Langley Research Center, Hampton, VA, 1994, pp. 603–619.
[6] Brot, A., "Probabilistic Inspection Strategies for Minimizing Service Failures," *FAA/NASA International Symposium on Advanced Structural Integrity Methods for Airframe Durability and Damage Tolerance, NASA Conference, Part 1*, NASA Langley Research Center, Hampton, VA, 1994, pp. 99–109.
[7] Fujimoto, Y., Kim, S. C., Hamada, K., and Huang, F., "Inspection Planning Using Genetic Algorithm for Fatigue Deteriorating Structures," *Proceedings of the International Offshore and Polar Engineering Conference*, Vol. 4, International Society of Offshore and Polar Engineers, Golden, CO, 1998, pp. 461–468.
[8] Toyoda-Makino, M., "Cost-Based Optimal History Dependent Strategy for Random Fatigue Cracks Growth," *Probabilistic Engineering Mechanics*, Vol. 14, No. 4, Oct. 1999, pp. 339–347.
[9] Enright, M. P., and Frangopol, D. M., "Reliability Based Lifetime Maintenance of Aging Highway Bridges," *Proceedings of SPIE 5th International Symposium on Nondestructive Evaluation and Health Monitoring of Aging Infrastructure*, International Society of Optical Engineers, Bellingham, WA, 2000, pp. 4–13.
[10] Wu, J. Y., Millwater, R. Y., Enright, M. P., Chell, G. G., Kuhlman, C. J., and Leverant G. R., "Probabilistic Method for Design Assessment of Reliability with Inspection (DARWIN)," AIAA Paper 00-1371, 2000.
[11] Garbatov, Y., and Soares, C. G., "Cost and Reliability Based Strategies for Fatigue Maintenance Planning of Floating Structures," *Reliability Engineering and System Safety*, Vol. 73, No. 3, 2001, pp. 293–301.
[12] Wu, J., and Shin, Y., "Probabilistic Damage Tolerance Methodology for Reliability Design and Inspection Optimization," AIAA Paper 04-1789, 2003.
[13] Wu, J., and Shin, Y., "Probabilistic Function Evaluation System (ProFES) for Maintenance Optimization," AIAA Paper 2005-2214, 2005.
[14] Hellevik, S. G., Langen, I., and Sørensen, J. D., "Cost Optimal Reliability Based Inspection and Replacement Planning of Piping Subjected to CO_2 Corrosion," *International Journal of Pressure Vessels and Piping*, Vol. 76, No. 8, 1999, pp. 527–538.
[15] Backman, B., "Structural Design Performed to Explicit Safety Criteria Containing Uncertainties," AIAA Paper 01-1241, 2001.
[16] Harkness, H. H., "Computational Methods for Fracture Mechanics and Probabilistic Fatigue," Ph.D. Dissertation, Dept. of Mechanical Engineering, Northwestern Univ., Evanston, IL, 1994.
[17] Kale, A. A., Haftka, R. T., Papila, M., and Sankar, B. V., "Tradeoff for Weight and Inspection Cost for Fail-Safe Design," AIAA Paper 2003-1501, 2003.
[18] Kale, A. A., Haftka, R. T., and Sankar, B. V., "Tradeoff of Structural Weight and Inspection Cost in Reliability Based Optimum Design Using Multiple Inspection Types," AIAA Paper 2004-4404, 2004.
[19] Lin, K. Y., Rusk, D. T., and Du, J., "An Equivalent Level of Safety Approach to Damage Tolerant Aircraft Structural Design," AIAA Paper 00-1371, 2000.
[20] Sinclair, G. B., and Pierie, R. V., "On Obtaining Fatigue Crack Growth Parameters From the Literature," *International Journal of Fatigue*, Vol. 12, No. 1, 1990, pp. 57–62.
[21] "Joint Service Specification Guide," Department of Defense, 1998.
[22] Niu, M., C., "Airframe Structural Design," *Fatigue, Damage Tolerance and Fail-Safe Design*, Conmilit Press, Hong Kong, 1990, pp. 538–570.
[23] Palmberg, B., Blom, A. F., and Eggwertz, S., "Probabilistic Damage Tolerance Analysis of Aircraft Structures," *Probabilistic Fracture Mechanics and Reliability*, M. Nijhoff, Dordrecht, The Netherlands, 1987.
[24] Rummel, W. D., and Matzkanin, G. A., *Nondestructive Evaluation Capability Data Book*, 3rd ed., Nondestructive Testing Information Analysis Center, Austin, TX, 1997.
[25] Tober, G., and Klemmt, W. B., "NDI Reliability Rules Used by Transport Aircraft-European View Point," *15th World Congress on Non Destructive Testing*, Daimler-Benz Aerospace Airbus GmbH, Paper 739, Rome, Italy, Oct. 2000.
[26] Kale, A. A., Haftka R. T., and Sankar B. V., "Reliability Based Design and Inspections of Stiffened Panels," AIAA Paper 2005-2145, 2005.
[27] ARENA, Ver. 3.01., System Modeling Corporation, Milwaukee, WI, 1997.
[28] Venter, G., "Non-Dimensional Response Surfaces for Structural Optimization with Uncertainty," Ph.D. Dissertation, Dept. of Mechanical and Aerospace Engineering, Univ. of Florida, Gainesville, FL., 1998.
[29] Petit, R. G., Wang, J. J., and Toh, C., "Validated Feasibility Study of Integrally Stiffened Metallic Fuselage Panels for Reducing Manufacturing Costs," NASA CR-2000-209342, 2000.